Preprint typeset in JINST style - HYPER VERSION

Development of a Scintillation Detector using a MPPC as an Alternative to an APD

Takamasa Miura[a]*, Takeshi Nakamori[a], Jun Kataoka[a], Takuya Kato[a], Kenichi Sato[b], Yoshitaka Ishikawa[b], Kazuhisa Yamamura[b], Nobuyuki Kawabata[b]

[a]*Research Institute for Science and Engineering, Waseda University, 3-4-1 Ohkubo Shinjuku Tokyo, Japan*
[b]*Solid State Division, Hamamatsu Photonics K. K., 1126-1 Ichino-cho Hamamatsu Shizuoka, Japan*
E-mail: `miura-tkms.eijo@toki.waseda.jp`

ABSTRACT: We conducted a study to examine the performance of the multi-pixel photon counter(MPPC). The MPPC is a novel type of semiconductor photodetector consisting of multiple avalanche photodiode (APD) pixels operated in Geiger mode. Whereas the MPPC offers a great advantage in signal multiplication comparable to that achieved by the photomultiplier tube (PMT), the detection of weak scintillation light signals is difficult due to the severe contamination of dark counts. In this study, we first compared the energy resolutions and energy thresholds of a 3×3 mm^2 MPPC with those of a 3×3 mm^2 APD as scintillation detectors. The MPPC and APD were optically coupled with $5\times5\times5$ mm^3 scintillation crystals of BGO, Tl:CsI, Pr:LuAG, and YAG. It turned out that the APD had better energy resolutions for 662 keV gamma-rays, while the MPPC had lower energy thresholds as measured using a test pulse. Despite the low energy thresholds, it is difficult for the MPPC to detect low energy gamma-rays due to the contamination of dark counts. Secondly, we applied a coincidence technique to discriminate weak gamma-ray signals from dark counts by using scintillation detectors that consisted of a 2×2 MPPC-array optically coupled with $10\times10\times10$ mm^3 crystals of GSO, BGO, and Pr:LuAG. With this technique, we demonstrated that dark counts achieved a rejection efficiency of more than 99.8%. As a result, 22.2 keV gamma-rays were successfully detected with a GSO scintillator as measured at $+20$ °C.

KEYWORDS: Gamma-rays; Scintillation detector; MPPC; Avalanche photodiode; Coincidence.

*Corresponding author.

Contents

1. Introduction

A Multi-Pixel Photon Counter (MPPC), also known as a Silicon Photo-Multiplier (SiPM), is a compact, high performance semiconductor photodetector comprising numerous Geiger mode avalanche photodiode (APD) pixels. In particular, MPPC offers great advantages such as low bias voltage operation (typically $\sim$70 V), high gain (10^{5-6}) almost comparable to conventional photomultiplier tubes (PMTs) and imperviousness to magnetic fields [1]-[3]. However, one of its weak points is the limited number of pixels, resulting in the nonlinear response of output signals. Each APD pixel has "dead time" (typically $\sim afew10$ nsec) once the Geiger discharge has triggered, namely, where multiple photons entering a single pixel cannot be counted within the dead time. Moreover, thermal electrons also trigger Geiger discharge, resulting in substantial contamination of "dark counts", which typically amounts to 1–4 Mcps for 3×3 mm^2 MPPCs (25μm type) measured at room temperature (+25°C) [1]-[3]. Nevertheless, its compactness and high gain are relatively attractive in various fields of high energy physics. For instance, MPPCs will be implemented as a photo sensor to determine weak scintillation light signals in the T2K experiment in order to measure the neutrino oscillation [4]. The use of compact semiconductor photodetectors like MPPC and APD, rather than traditional PMTs, are also promoted in various other ways as described below.

X-ray and gamma-ray astronomical satellites often carry various scintillators, not only as main detectors but also active shields, which effectively reduce background events caused by charged particles (including geomagnetically trapped particles and primary cosmic rays) as well as atmospheric gamma-rays. For instance, the hard X-ray detector (HXD) [5] onboard Suzaku (launched in 2005)[6] utilizes $Bi_{12}Ge_3O_{20}$ (BGO) crystals as the active shield for a phoswich detector. 36 PMTs were implemented in the HXD, but semiconductor photodetectors, if applicable, can easily replace such bulky systems by saving *both* space and power. Firmly motivated, a Tokyo Tech pico-satellite, Cute1.7+APD II, validates the inaugural use of APDs as a radiation detector in a space experiment [7]. The Astro-H, which is a Japanese X-ray astronomy satellite alongside Suzaku to be launched in 2014, will carry 68 APDs to read out shield BGO crystals both in the hard X-ray imager (HXI) and soft gamma-ray detector (SGD) [8]. These APDs are linear mode devices operating with only a moderate gain of $50-100$, thus making it difficult to achieve energy thresholds as low as 50 keV. In this context, MPPC could be a promising device to replace the APD and further extend the energy coverage of scintillation detectors.

Positron Emission Tomography (PET), another good example of MPPC application, is a well-established method for diagnosing locational and active information on cancers within human bodies or in animals [9]. Conventional PET detectors consist of hundreds of PMTs with pixelized inorganic scintillators like $Lu_2(SiO_4)O$ (LSO), $Gd_2(SiO_4)O$ (GSO) and BGO. PET combined with computed tomography (PET/CT) is currently most popular, but CT imaging suffers from poor soft-tissue contrast, with patients also subjected to a significant radiation dose that exceeds that received from the PET itself. In contrast, magnetic resonance imaging (MRI) offers excellent soft-tissue contrast and anatomical detail without the additional radiation. Unfortunately, PMT is difficult to use within the MRI high magnetic field of $a few$ T, hence efforts to replace the PMT with APD or MPPC have been actively studied in literature [10]-[12]. Moreover, MPPC offers excellent timing resolution thanks to its high gain. A combination of MPPC with brand-new scintillators with excellent light output and/or fast timing properties is being investigated for future application in a Time-Of-Flight (TOF) PET scanner [13]. Pr-doped $Lu_3Al_5O_{12}$ (Pr:LuAG) [14],[15] is one such scintillator characterized by its very rapid decay, high density and high light yield. Its performance with UV-enhanced APD array is already reported elsewhere [15].

Dark counts of MPPC can be severely problematic for all applications and hence should be suppressed as far as possible to ensure optimal detector performance. The idea of rejecting $>$ 99 % of dark counts was suggested by Bencardino et al.(2010)[16], featuring an anti-coincidence technique where two MPPCs were stuck to a single plastic scintillator and triggers were generated when both MPPCs fired at the same time.

In this paper, we examined the potential of whether MPPCs could replace APDs as a component of wide band scintillation detectors. We compared the energy resolutions and energy thresholds of the MPPC with those of the APD by using four scintillators BGO, Tl:CsI, Pr:LuAG, and YAG crystals. We also applied the coincidence technique to improve the energy thresholds using a large-area, monolithic 2×2 MPPC array coupled with GSO, BGO, and Pr:LuAG scintillators.

2. Comparison of Performance

First, we examined the performance of scintillation detectors consisting of either the MPPC or APD. All data were taken at 20 °C and the setup of the experiments is outlined below.

The 3×3 mm^2 MPPC S10362-33-025C (shown in the center of Figure 1) and the 3×3 mm^2 APD S8664-33-8825(X) (shown on the left in Figure 1) from Hamamatsu were selected. The operational gains were 2.75×10^5 for the MPPC and 50 for the APD. The dark count rate of the MPPC was 2.40 Mcps; the dark current of the APD was 1.81 nA. The MPPC (or the APD) was optically coupled with 5×5×5 mm^3 scintillators (BGO, Tl:CsI, Pr:LuAG, and YAG) using silicone optical grease (OKEN6262A), and then wrapped in Teflon tape. Signals from the MPPC (or the APD) were fed into a preamplifier (ClearPluse 595H with 560 pF feedback capacitor for the MPPC or ClearPluse 580K with 1 pF feedback capacitor for the APD), a shaping amplifier (ORTEC 570; shaping time of 2 μsec), and then digitized by a multichannel analyzer (Amptek MCA8000A). Signals from a test pulse (Berkeley Nucleonics Corp. PB-5) were also fed into the preamplifier, with FWHM of test pulse peaks being used for defining the energy thresholds.

Figure 2 shows the energy spectra obtained with various scintillators. For instance, with the BGO scintillator, the FWHM energy resolutions of 662 keV gamma-rays are 23.7 % and 19.8 % for the MPPC and APD, respectively. The energy thresholds are 21.6 keV for the MPPC and 39.2 keV for the APD. Table 1 lists the other results,which suggests that the APD achieves better energy resolution, while the MPPC achieves lower energy threshold. Although the MPPC has lower energy thresholds than those of the APD, it is quite difficult for the MPPC to detect low energy gamma-rays as shown in Figure 2. This difficulty may be due to the dark counts that generate a charge comparable to that of a few scintillation photons. Because the gamma-ray event rate was up to 10 kcps in this measurement, the peak of low energy gamma-rays was hidden behind the contamination of dark counts at a the rate of $\sim$2.4 Mcps. In order to improve the signal-to-noise ratio for low energy gamma-rays, we applied a coincidence technique for a scintillation detector equipped with a 2$\times$2 MPPC array as described in the following section.

3. Detecting Gamma-rays with the Coincidence Technique

The setup of measurements is initially described, followed by an overview of the system in Figure 3. For this experiment, the monolithic 2$\times$2 MPPC array S10985-025C from Hamamatsu (Figure 1, *right*) was selected. Each MPPC pixel was 3×3 mm^2, comprising a 120×120 Geiger mode APD matrix arranged with a pitch of 25 μm. The dark count rate of each MPPC pixel (3×3 mm^2) was 900 kcps with a gain of 2.75×10^5 measured at 20 °C.

The MPPC array and the scintillators were optically coupled using silicone optical grease (OKEN N6262A) and a scintillator and MPPC array were wrapped as a whole, using Teflon tape. The output signals from each of the MPPC pixels were multiplied by a factor of 100 using a fast current amplifier (Phillips 6954) and then inverted/divided by Quad linear FAN IN/OUT (Phillips 740). One of the divided signals was directly fed into the charge sensitive ADC (HOSHIN V005) after a 100 nsec delay (using Technoland N-TS 100), whereas another signal was used to make a gate for the ADC. The threshold level of the discriminator (Technoland N-TM 405) was set to 0.5 $\sim$ 1 p.e. level, and the output width was set to 75 nsec, the maximum length with this module. Before making the final ADC gate, the coincidence among 1 to 4 MPPC channels was determined using a coincidence module (Kaizu Works KN470), and adjusted by a gate and delay generator (Technoland N-TM 307). A common bias voltage was supplied to each MPPC pixel by KEITHLEY 2400, corresponding to a gain of 2.75×10^5. All the data were taken at +20 °C.

Before taking the data, the ADC gate width was carefully optimized. Apparently, the wider ADC gate can contain a greater fraction of the charge signals from the scintillator, but meanwhile, the increased dark count will contaminate. The signal-to-noise ratio was thus scanned as a function of gate width, before searching for the optimal value allowing the lowest energy threshold when measured with 662 keV gamma-rays. Consequently, it was concluded that the optimal width for the ADC gate should be 200 nsec for GSO and Pr:LuAG, and 500 nsec for the BGO, respectively, as measured at room temperature (+20 °C).

First, details of how effectively the coincidence technique works to reduce the dark counts are presented, by irradiating 60 keV gamma-rays from ^{241}Am on the GSO scintillator. Figure 4 compares the energy spectra taken with various numbers of coincidence channels, from 1 (triggered only by a single channel, i.e. without coincidence) to 4 (coincidence of all channels). A prominent peak at around 5 keV is due to the dark counts. It is apparent that the coincidence technique drastically reduces the dark counts, where the background trigger rate derived from the dark counts decreases from 9.0×10^2 kcps (without the coincidence) to 1.4×10^2, 1.9×10 and 1.7 kcps with 2-, 3-, and 4-fold coincidences, respectively. In particular, when the 4-fold coincidence is applied, the dark count is effectively reduced with an rejection efficiency of > 99.8 %. The energy resolutions for 59.5 keV gamma-rays of each spectrum are 60 ± 3 % (FWHM), where the peak position and energy resolution may not be significantly affected by the dark count contamination.

Next, an energy spectrum of ^{137}Cs was measured using this coincidence technique. The spectra with the GSO are shown in Figure 5, in which the solid and dashed lines represent 4-fold coincidence and no coincidence respectively. The FWHM energy resolutions are both 15.0 ± 0.1 % for 662 keV. With the coincident triggers, as well as 662 keV gamma-rays, the 32 keV K_α X-ray peak could also be very clearly detected, while this low energy peak was heavily diluted by the dark count and inevitably smoothed out without the coincidence technique. The result successfully demonstrates a significant improvement in the signal-to-noise ratio at the lowest energy range of the scintillation detector.

The energy spectra of ^{137}Cs were also measured with the BGO and Pr:LuAG on the 2×2 MPPC array using the coincidence technique. The spectra obtained are shown in Figure 6 with the GSO spectrum for comparison. Although the 32 keV X-ray peak can be identified in the GSO spectrum, neither the BGO spectrum nor Pr:LuAG shows this peak. These results are discussed in the following section. The energy resolutions (FWHM) of 662 keV were 18.4 ± 0.1% (BGO), and 23.8 ± 0.1% (Pr:LuAG). **The energy resolution of Pr:LuAG for 662 keV gamma-rays is worse than 14.70 % as reported by Kato et al.(2011)[12]. This worse efficiency in collecting scintillation photons was attributed to two reasons: First, the area covered by the MPPC was too narrow. In this study, a $10\times10\times10$ mm^3 Pr:LuAG crystal was coupled to a 2×2 MPPC array having a total active area of 6×6 mm^2, while a $3\times3\times10$ mm^3 crystal was read out by a 3×3 mm^2 MPPC in the previous study. The second reason is that the Teflon tape used in this study is less reflective with $\sim$310 nm scintillation light of Pr:LuAG than $BaSO_4$[17] used in the previous study. It should be possible to improve the 662 keV energy resolution by increasing the efficiency of photon collection.**

Finally, 22 keV gamma-rays were measured from ^{109}Cd with the GSO, in which the coincidence technique worked most effectively. The spectra are shown in Figure 7, whereby the solid and dashed lines correspond to the spectrum taken with and without the 4-fold coincidence, respectively. The 22 keV gamma-ray peak was clearly detected by the coincidence and energy resolution of 63 ± 4 % (FWHM). Therefore the energy threshold of the GSO with the MPPC array was proved to be $\simeq$10 keV.

4. Conclusions and Discussions

In this study, we quantitatively compared the energy resolutions and energy thresholds of a MPPC with those of an APD as scintillation detectors. We also employed a coincidence technique with a 2×2 MPPC array and then effectively rejected dark noise. The APD proved favorable in terms of energy resolution, while the MPPC was superior in terms of energy threshold. Despite the MPPC's superiority regarding the energy threshold, the peak of low energy gamma-rays was critically smoothed out by the dark counts. However, the coincidence technique reduced the contamination of dark counts with an efficiency exceeding 99.8 %; consequently, 22.2 keV gamma-rays were successfully detected with GSO at $+20$ °C.

With regard to energy resolution, a photon detection efficiency (PDE) would be the dominant factor. PDE is equivalent to the quantum efficiency (Q.E.) for the APD, which typically exceeds 80 % at around 500–800 nm, while that of the MPPC is much less than the Q.E. due to a low aperture ratio of $\sim$30 % for the 25 μm pitch type [1]. For these statistical reasons, better energy resolutions were obtained with the APD. Conversely, the energy thresholds may depend mainly on the amount of charge generated, and thus, the MPPC offers a great potential capacity for low energy thresholds due to its superior signal multiplication. The dark counts, however, contaminated the low energy region of the spectra and interfered with the detection of low energy gamma-rays.

With the coincidence technique for the GSO scintillator, we defined the energy threshold in the following way. Because 490 photoelectrons were detected with the 662 keV gamma-rays, it can be assumed that 1 photoelectron corresponds to 1.35 keV. Thus, with the 4-fold coincidence, the energy threshold corresponds to 1.35×4 = 5.4 keV of gamma-rays. In the same way, it turned out to 8.0 keV for the BGO and 10.2 keV for the Pr:LuAG.

In the case with the BGO, the 32 keV X-ray peak could hardly be detected, probably because the long BGO decay, the gate width should be correspondingly extended, which hampers efforts to exclude dark count contamination.

For the Pr:LuAG, the intrinsic background derived from ^{176}Lu, which emits electrons in beta decay, must be considered, since the spectrum of Pr:LuAG contains not only gamma-ray but also electron background events (see Figure 6). Moreover, the quantity of photoelectrons detected by 662 keV gamma-rays is not comparable to that with the GSO, though the Pr:LuAG yields more than twice as many photons as the GSO. Accordingly, as with the BGO, 32 keV X-rays could not be detected clearly. The major cause is the fact that the peak wavelength of Pr:LuAG is 310 nm, at which the photon detection efficiency of the MPPC is less than 10 %. Such disadvantage is mainly due to epoxy resins conventionally used as the window of APDs. Besides, the Teflon tapes are not particularly reflective for UV light, meaning the scintillation light from Pr:LuAG cannot be collected efficiently. Yoshino, et al.[15] developed UV-enhanced APD, which significantly improved the quantum efficiency by $\sim$ 10 times at the Pr:LuAG peak wavelength. We expect the development of UV-enhanced MPPC to achieve much better performances with Pr:LuAG, in term of both energy resolution and lower energy detectability.

Acknowledgments

We thank the anonymous reviewers for their helpful comments, which helped to clarify many issues presented in this paper.

References

[1] S.Gomi et al., *Development of multi-pixel photon counters, I*EEE Trans. Nucl. Sci.**N30-108** (2006) 1105.

[2] K.Yamamoto et al., *Development of multi-pixel photon counter (MPPC), I*EEE Trans. Nucl. Sci.**N24-292** (2007) 1511.

[3] D.J.Herbert et al., *First results of scintillator readout with silicon photomultiplier, I*EEE Trans. Nucl. Sci.**53** (2006) 389.

[4] A. Vacheret, *Characterization of the 1.3 mm × 1.3 mm MPPC for the T2K near detectors N*ucl. Instrum. Methods Phys. Res., Sect. A**623** (2010) 201.

[5] T.Takahashi et al., *Hard X-ray detector (HXD) on board Suzaku P*ubl. Astro. Soc. J.**59** (2007) 35.

[6] K.Mitsuda et al., *The X-ray observatory Suzaku P*ubl. Astro. Soc. J.**59** (2007) 1.

[7] J.Kataoka et al., *In-orbit performance of avalanche photodiode as radiation detector on board the picosatellite Cute-1.7+APD II J*. Geophys. Res.**115** (2010) A05204.

[8] T.Takahashi et al., *The ASTRO-H mission P*roc. SPIE**7732** (2010) 77320Z-1

[9] W.W.Moses, *Trends in PET imaging N*ucl. Instrum. Methods Phys. Res., Sect. A**471** (2001) 209.

[10] J.Kataoka et al., *Development of an APD-based PET module and preliminary resolution performance of an experimental prototype gantry I*EEE Trans. Nucl. Sci.**57** (2010) 2448.

[11] A.Nassalski et al., *Multi pixel photon counters (MPPC) as an alternative to APD in PET applications I*EEE Trans. Nucl. Sci.**57** (2010) 1008.

[12] K.Kato et al., *Development of a large-area monolithic 4×4 MPPC array for a future PET scanner employing pixelized Ce:LYSO and Pr:LuAG crystals N*ucl. Instrum. Methods Phys. Res., Sect. A**638** (2011) 83.

[13] G.-C.Wang, *Timing optimization of solid-state photomultiplier based PET detectors I*EEE Trans. Nucl. Sci.**57** (2010) 25.

[14] K.Kamada et al., *Scintillation properties of 2-inch-diameter* $Pr{:}Lu_3Al_50_{12}$ *(LuAG) single crystal I*EEE Trans. Nucl. Sci.**56** (2009) 570.

[15] M.Yoshino et al., *The development and performance of UV-enhanced APD-arrays for high resolution PET imaging coupled with pixelized Pr;LuAG crystal N*ucl. Instrum. Methods Phys. Res., Sect. A.**643** (2011) 57.

[16] R.Bencardino et al., *Anti-coincidence rejection of SiPM dark pulses for improved detection of low energy radiation N*ucl. Instrum. Methods Phys. Res., Sect. A**619** (2010) 497.

[17] K.Kamada et al., *Basic experiments on radiation imaging by using* $Pr{:}Lu_3Al_5O_{12}$ *(LuAG) small crystalline pixels with various reflector I*EEE Trans. Nucl. Sci.**N24-208** (2007) 1417.

Table 1. Performances of MPPC and APD with various scintillators

	FWHM energy resolutions of the 662 keV gamma-rays (%)		Energy thresholds (keV)	
	MPPC	APD	MPPC	APD
BGO	23.7	19.8	21.6	39.2
Tl:CsI	16.2	10.2	4.39	7.40
Pr:LuAG	21.3	14.0	14.9	23.9
YAG	20.3	18.9	11.8	22.0

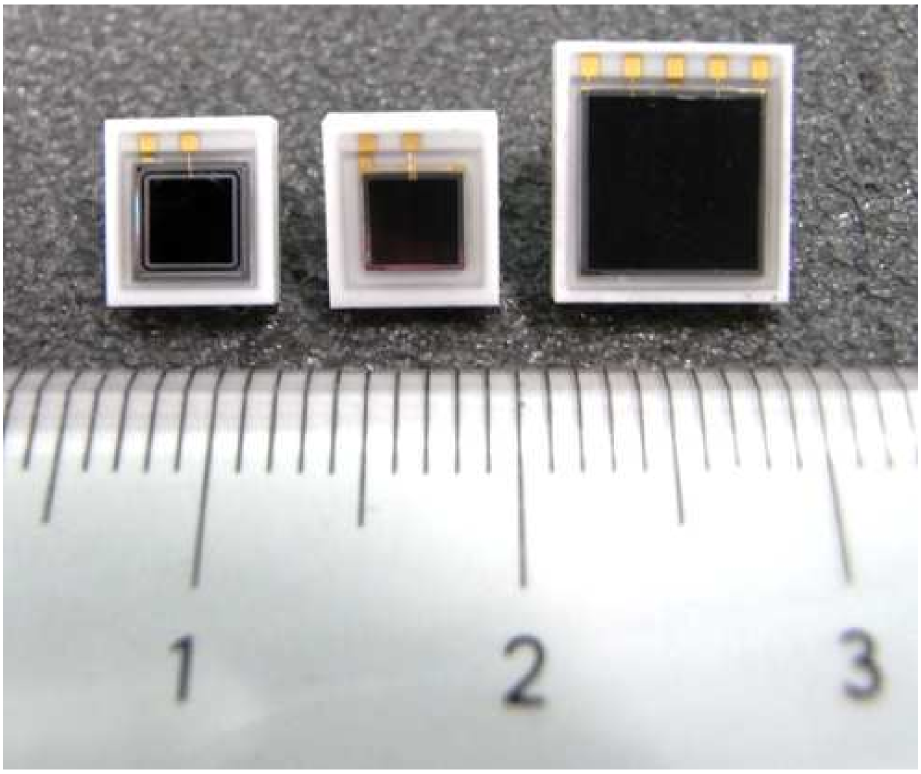

Figure 1. Photograph of the 3×3 mm^2 APD, the 3×3 mm^2 MPPC, and the 2×2 MPPC array, from left to right.

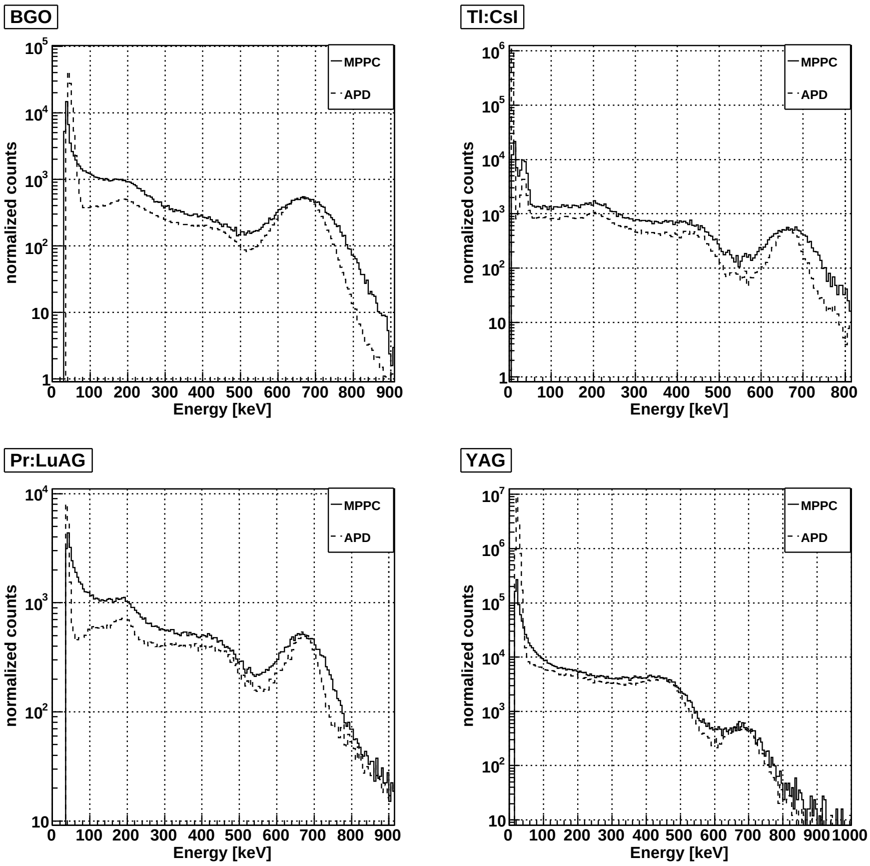

Figure 2. Energy spectra of the ^{137}Cs measured with the various scintillators (BGO at the top left, Tl:CsI at top right, Pr:LuAG at bottom left, and YAG at bottom right) at +20 °C. Each spectrum is normalized at the photoelectric absorption peak. Solid and dashed lines show the spectra with the MPPC and APD, respectively.

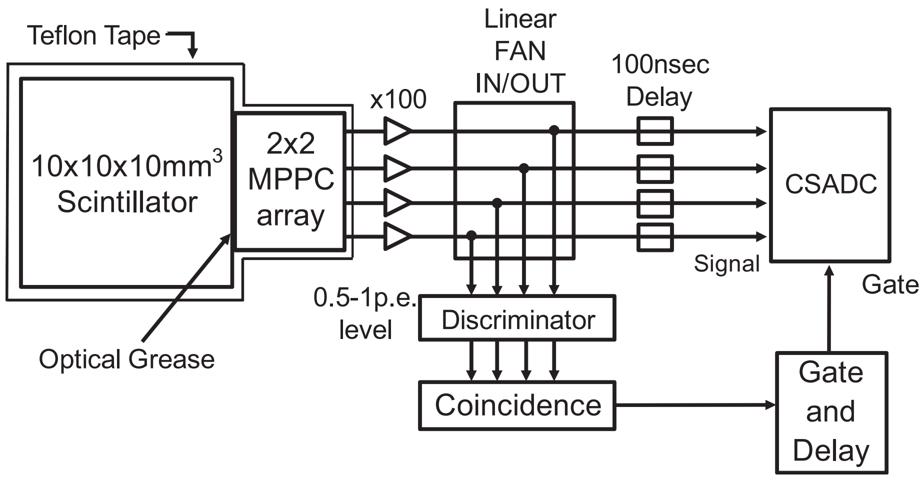

Figure 3. Diagram of the readout system.

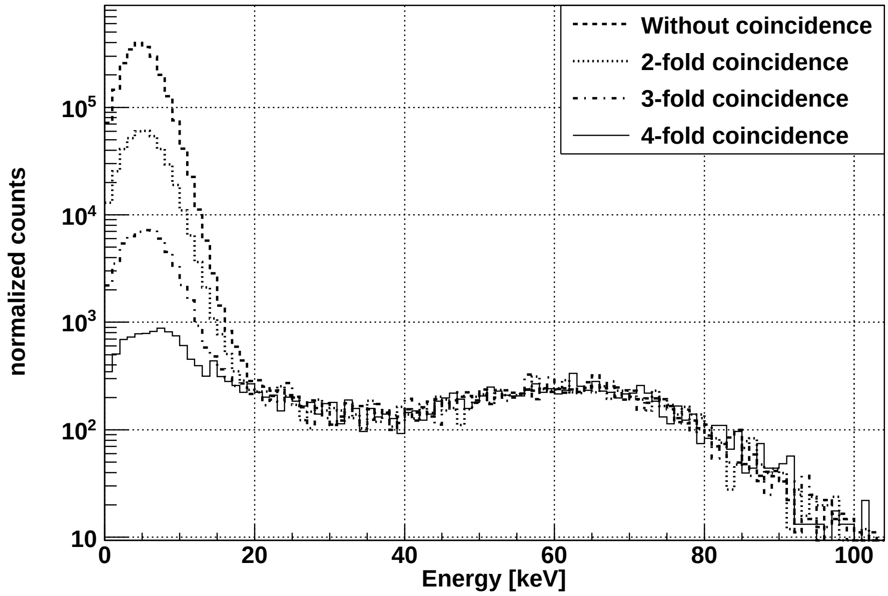

Figure 4. Energy spectra of the ^{241}Am measured with the GSO at $+20\ ^{\circ}$C for the different trigger conditions (see text). Each spectrum is normalized at the photoelectric absorption peak. The dashed line shows the spectrum without the coincidence trigger while dotted, dot-dashed and solid lines correspond to 2-, 3- and 4-fold coincident events respectively.

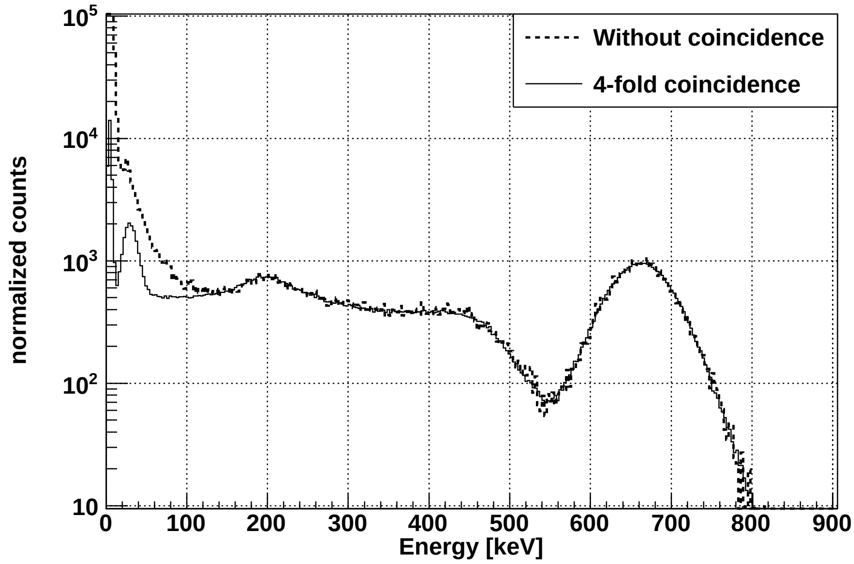

Figure 5. Energy spectra of ^{137}Cs measured with the GSO at $+20\ ^{\circ}$C. Solid and dashed lines correspond to cases with and without the coincidence respectively.

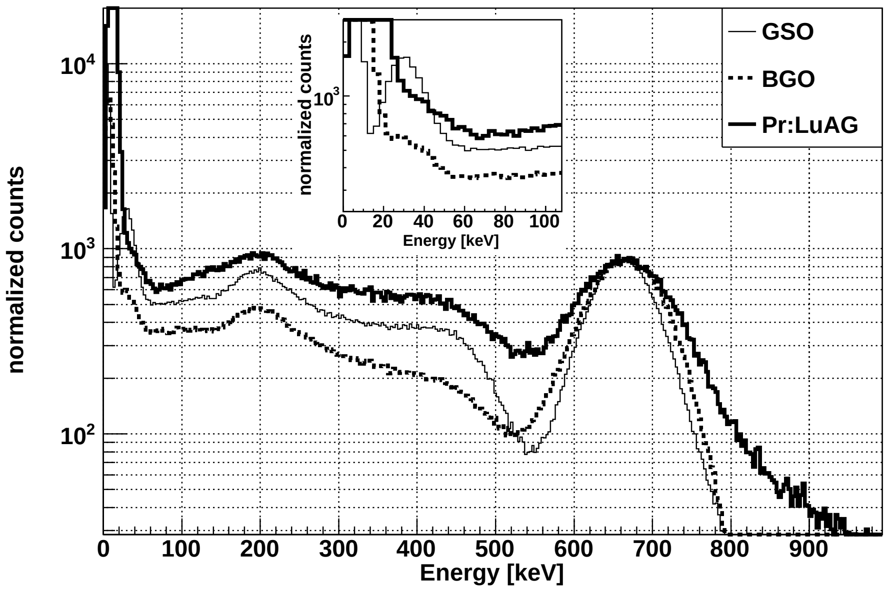

Figure 6. Energy spectra of ^{137}Cs measured with the three scintillators on 2×2 MPPC array with the 4-fold coincidence. Solid, dashed and thick solid lines represent spectra with GSO, BGO, and Pr:LuAG, respectively. The inset panel is a close-up view around 32 keV peaks.

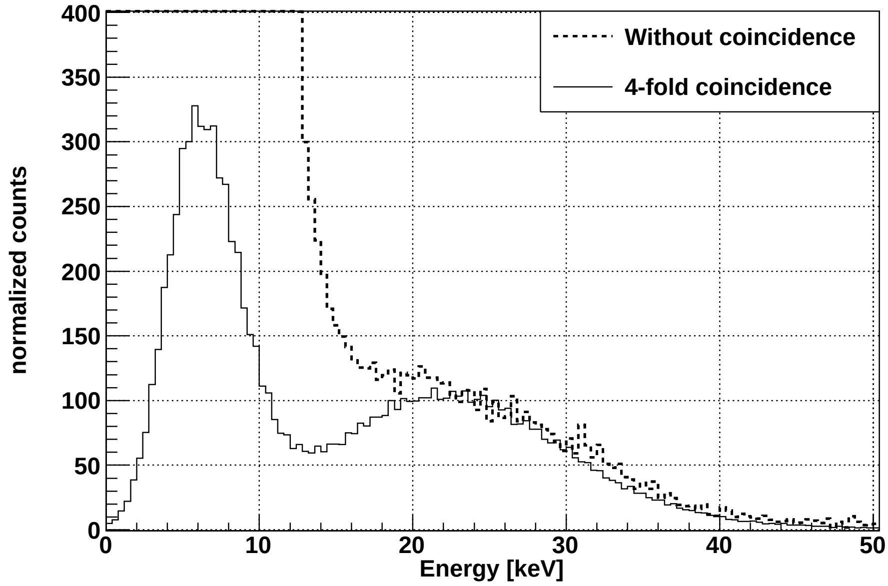

Figure 7. ^{109}Cd gamma-ray spectra with the GSO at +20 °C. Solid and dashed lines correspond to cases with and without the coincidence respectively.